Use of Single Star Sightings in Boost Navigation

CORNELIUS T. LEONDES*
University of California, Los Angeles
AND
JEFFREY M. NASH†
Logicon, Inc., San Pedro, Calif.

Information obtained from a single inflight star sighting is used to calibrate a boost vehicle's IMU errors. Several error-inducing parameters, including initial alignment, accelerometers, and gyros are included in the estimation state vector. Although the problem studied is shown to be generally unobservable, suitable preflight alignment techniques can be used to induce observability. The resultant induced observability arises from correlations between initial alignment errors and platform gyros or accelerometers used for initially aligning the platform. When the platform's initial misalignment is directly observable, the presence of correlations between the initial misalignment and formerly unobservable error sources permits estimation of the latter. Additional results and a sample problem demonstrate the effect of variations in initial conditions, dynamic effects, and observation noise as a function of relevant design parameters.

Introduction

THE simplicity of an inertial platform-mounted, single-star sighting device lends practical appeal to its use in boost navigation. In this article, the large-scale calibration of several platform misalignment-inducing error sources is considered.

Figure 1 is a schematic of the simple mechanization under consideration. A possible orientation is depicted. The single-star stellar inertial measurement unit, or SIMU, is discussed in Ref. 1. Typically, SIMUs are proposed for use in real-time flight azimuth estimation. Postulating the use of nominal, preflight-generated sensitivities, however, recursive minimum-variance filtering can be employed to achieve large-scale error source calibrations.

Equation Development

Assume that both the predicted and actual target star locations can be expressed as platform-to-star unit vectors in platform coordinates. If the difference between the predicted and observed unit vectors in platform coordinates is designated y_p, it is true that:‡

$$y_p = \hat{n}_{p_{(\text{predicted})}} - \hat{n}_{p_{(\text{observed})}} \tag{1}$$

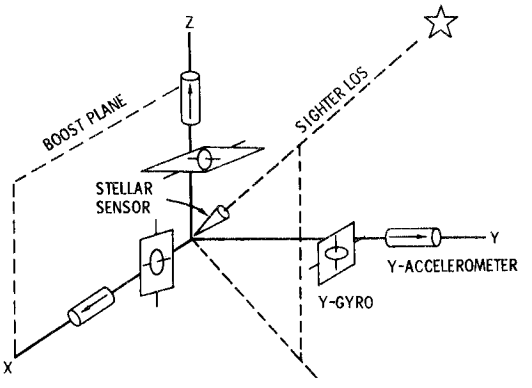

Fig. 1 Stellar inertial measurement unit.

Received May 1, 1974; revision received August 2, 1974. The research reported in this article was supported in part by the U.S. Air Force Office of Scientific Research under AFOSR Grant 72-2166.
Index category: Navigation, Control, and Guidance Theory.
* Professor, Engineering Systems Department. Member AIAA.
† Member of the Technical Staff, Systems Analysis Department.
‡ Note: use of italics denotes vectors; vector components are italicized and subscripted as appropriate.

The total observable is attributed to the set of three platform misalignments (ω_i) existing at the instant of sighting. Figure 2 depicts the relevant geometry which results in a nonzero y_p.

To facilitate application of linear estimation theory, it is desirable to express y_p in the form:

$$y_p = A\omega + n \tag{2}$$

where

$$\omega \triangleq \begin{bmatrix} \omega_x \\ \omega_y \\ \omega_z \end{bmatrix}$$

a (3×1) vector composed of the three instantaneous misalignments about each of the platform axes

$$A \triangleq [\partial y/\partial \omega],$$

(3×3) sensitivity matrix, and

$$n \triangleq a\,(3 \times 1)$$

random vector of sighter Gaussian noise described in platform coordinates by a (3×3) covariance matrix, R.

Returning to Eq. (1), an alternate expression for y_p is given as:

$$y_p = [P_M \leftarrow P_A][P \leftarrow I]\hat{n}_I - [P \leftarrow I]\hat{n}_I' \tag{3}$$

where $\hat{n}_I$ is the platform-to-star unit vector expressed in inertial coordinates. In an application, this vector is obtained as a function of nominal launch profile and stellar ephemeris data.

$[P \leftarrow I]$ is the nominal inertial-to-platform coordinate frame transformation matrix. In an actual application, this matrix is defined by the platform's initial alignment and the selection of an inertial frame.

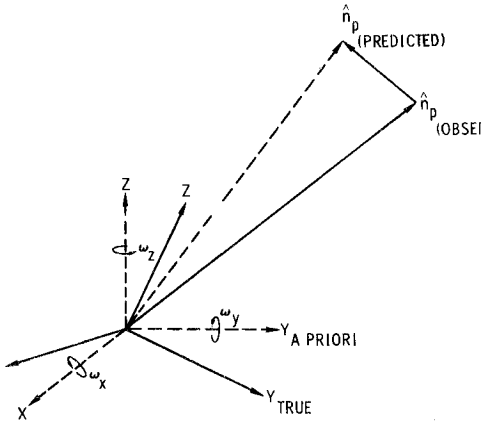

Fig. 2 Stellar observation geometry.

$[P_M \leftarrow P_A]$ is a small-angle rotation matrix consisting of three independent misalignments about each of the (nominal) platform's three axes. That is:

$$[P_M \leftarrow P_A] \triangleq \begin{bmatrix} 1 & \omega_z & -\omega_y \\ -\omega_z & 1 & \omega_x \\ \omega_y & -\omega_x & 1 \end{bmatrix} = [I] + [\varepsilon] \tag{4}$$

where

$$[\varepsilon] \triangleq \begin{bmatrix} 0 & \omega_z & -\omega_y \\ -\omega_z & 0 & \omega_x \\ \omega_y & -\omega_x & 0 \end{bmatrix}$$

Thus

$$y_p = \hat{n}_p + [\varepsilon]\hat{n}_p - \hat{n}_p = [\varepsilon]\hat{n}_p = [\varepsilon][P \leftarrow I]\hat{n}_I \tag{5}$$

Expanding the right-hand side of Eq. (5) and rearranging:

$$y_p = \begin{bmatrix} 0 & -n_{p_z} & n_{p_y} \\ n_{p_z} & 0 & -n_{p_x} \\ -n_{p_y} & n_{p_x} & 0 \end{bmatrix} \begin{bmatrix} \omega_x \\ \omega_y \\ \omega_x \end{bmatrix} \triangleq A\omega \tag{6}$$

The desired form, Eq. (6), is achieved with the A-matrix calculated as a strict function of the target star's nominal position, referenced to platform coordinates.

If it is additionally desired to estimate platform error sources individually, rather than the resultant aggregate misalignment set, additional sensitivities must be employed. Using techniques outlined in Ref. 2, one may generate the matrix B_k where:

$$B_k \triangleq [\partial\omega/\partial x]_k$$

$x \triangleq$ a vector of n navigation error parameters.

The generated matrix is assumed valid at the kth instant of flight along a nominal boost trajectory. Hence, Eq. (2) may be rewritten as:

$$y_{p_k} = A_k B_k x + n_k \equiv H_k x + n_k \tag{7}$$

where

$$H_k \triangleq A_k B_k$$

For the booster application considered here, it is assumed, over the relatively short time of vehicle flight, that the navigation error parameters (x) are constant but generally possess a zero-mean Gaussian component (ε) with covariance $Q(n \times n)$. A formulation of the minimum-variance, constant-parameter estimation algorithm is given (from Ref. 3, for example) as follows:

$$x_{k+1} = x_k + \varepsilon_k \tag{8}$$

$$y_{k+1} = H_{k+1}x_{k+1} + n_{k+1} \tag{9}$$

$$K_{k+1} = P_{\tilde{x}_k} H_{k+1}{}^T (H_{k+1} P_{\tilde{x}_k} H_{k+1}{}^T + R_{k+1})^{-1} \tag{10}$$

$$P'_{\tilde{x}_{k+1}} = P_{\tilde{x}_k} + Q_k \tag{11}$$

$$P_{\tilde{x}_{k+1}} = P'_{\tilde{x}_{k+1}} - K_{k+1} H_{k+1} P'_{\tilde{x}_{k+1}} \tag{12}$$

$$\hat{x}_{k+1} = \hat{x}_k + K_{k+1}(y_{k+1} - H_{k+1}\hat{x}_k). \tag{13}$$

The algorithm optimally updates and propagates estimates ($\hat{x}$) of the navigation state parameters (x). The algorithm's initiation requires initial estimates of both $P_{\tilde{x}_o} \triangleq E[(x_o - \hat{x}_o)(x_o - \hat{x}_o)^T]$ and $\hat{x}_o$.

Observability

The significance of observability in the boost navigation estimation problem stems from the necessity of complete observability in order to guarantee uniform asymptotic stability and convergence of the algorithm. Strictly defined, the constant-parameter estimation system, Eqs. (8–13), is completely observable over the estimation interval, $[k_o, k_f]$, if, for a given k_o and $k_f > k_o$, every state x can be determined from the knowledge of y_k over $[k_o, k_f]$.

The observability of a given message model is determined from the rank of the discrete-form symmetric Gramian matrix defined by:

$$G = \sum_{k=1}^{N} H_k{}^T H_k = \sum_{k=1}^{N} B_k{}^T A_k{}^T A_k B_k \triangleq \sum_{k=1}^{N} G_k \tag{14}$$

where H_k is that defined in Eq. (7). If G is of full rank, (i.e., $|G| \neq 0$) the message and estimation system associated with Eqs. (8–13) is completely observable. If it is postulated that the number of system error parameters is at least 3, by definition of A, B and ω, it is evident that the expression:

$$G_k = B_k{}^T A_k{}^T A_k B_k \tag{15}$$

can have at most rank 3. Further assuming that B_k is of full rank, the rank of G_k is solely dependent upon A_k where:

$$y_k = A_k \omega_k \tag{16}$$

and A is defined by Eq. (6). But, by inspection, rank $A = 2$; hence, rank $H = 2$. Because the single-star sighter is permitted to sight on but one star, the set $\{G_k : k = 1, \ldots, N\}$ is constant valued and the test imposed by Eq. (14) is failed. The stellar sighting-platform misalignment estimation problem, when restricted to a sighting on but one star, is therefore unobservable if more than 2 orthogonal misalignments are estimated.

For constant-parameter estimation problems, if $Hx = o \neq x = o$, those states for which the implication does not hold are classified as unobservable by application of Eq. (14). However, with suitable initial correlations, uncertainty reduction is achieved for unobservable states. The nature of correlation-induced observability is illustrated via example.

Let the state and observation models of Eqs. (8–9) hold. I.e., let:

$$y = y \triangleq (1 \times 1); \quad x \triangleq \begin{bmatrix} x_1 \\ x_2 \end{bmatrix}; \quad n = \mathbf{n} \triangleq (1 \times 1)$$

$$H_i = [1 \ 0](i = 1, \ldots, N) \tag{17}$$

Therefore

$$G = \sum_{i=1}^{N} H_i{}^T H_i = \begin{bmatrix} N & 0 \\ 0 & 0 \end{bmatrix}; \qquad |G| = 0 \tag{18}$$

$$|G| = 0 \tag{19}$$

Also

$$P_0 \triangleq \begin{bmatrix} P_{11} & P_{12} \\ P_{21} & P_{22} \end{bmatrix}; \qquad R_0 = \sigma_n{}^2 = E(n^2) \tag{20}$$

$$Q \equiv [0](2 \times 2); \qquad E(n) = 0 \tag{21}$$

After executing one iteration of the minimum variance algorithm, P_1 may be calculated:

$$P_1 = \begin{bmatrix} p_{11} - p_{11}{}^2/(\sigma_r{}^2 + p_{11}) & p_{12} - p_{11}p_{12}/(\sigma_r{}^2 + p_{11}) \\ p_{12} - p_{11}p_{12}/(\sigma_r{}^2 + p_{11}) & p_{22} - p_{12}{}^2/(\sigma_r{}^2 + p_{11}) \end{bmatrix} \tag{22}$$

In the limit, where the observation noise becomes negligibly small,

$$\lim_{\sigma_r{}^2 \to 0} P_1 = \begin{bmatrix} 0 & 0 \\ 0 & p_{22} - p_{12}{}^2/p_{11} \end{bmatrix} \tag{23}$$

which does not converge unless

$$p_{12} = (p_{11}p_{22})^{1/2} \Rightarrow (p_{12}/p_{11}p_{22})^{1/2} = 1 \tag{24}$$

which is the condition for perfect correlation between the two states x_1 and x_2. By induction on the example, this result is extended to unobservable, observable-correlated states in general. Thus, error covariance convergence can be assured by the provision of a suitable initial error covariance matrix; i.e., one which is nonsingular. Gura[4] has also noted the role of initial covariance matrices in somewhat more general problems.

A final aspect of the observability criterion, Eq. (14), requires attention. For the boost problem, H was shown to have rank 2. Since H^TH can have at most rank 2, the observability criterion will not be met for $n > 2$. Nonetheless, estimation of desired error source states is made possible by insuring that each error is correlated with at most 2 other sources. This requirement is tantamount to reducing the error covariance matrices to a set of 3×3 blocks. The reduced blocks can be processed iteratively or simultaneously with the same effect. The enforced reduction insures that block-by-block subproblem observability results in overall problem observability.

Table 1 Initial values of error source groups for standard case

Group number	Designation	RSS of 3 values	Units
	Accelerometers:		
1	Bias	3.46×10^{-5}	g
2	Linear scale factor	6.93×10^{-5}	g/g
3	Quadratic scale factor	1.73×10^{-5}	g/g^2
4	Cubic scale factor	3.46×10^{-5}	g/g^3
5	Cross axis bias	1.73×10^{-5}	g/cross g
6	Cross axis nonlinearity	1.73×10^{-5}	g/cross g
7	Secondary cross axis bias	1.73×10^{-5}	g/g/cross g
8	Secondary cross axis	1.73×10^{-5}	g/g/cross g
	Gyros:		
9	Fixed drift	1.73	deg/hr
10	Spin axis mass unbalance	1.73	deg/hr/g
11	Input axis mass unbalance	1.73	deg/hr/g
12	Anisoelasticity	3.46×10^{-2}	$deg/hr/g^2$
	Platform:		
13	Initial misalignments	360.3	arc sec
14	Servo errors	17.3	arc sec
15	*P*-deformation	17.3	arc sec/g
16	*Q*-deformation	1.73	arc sec/g
	Launch Point:		
17	Initial position	1.73	ft
18	Initial velocity	0	fps

Sample Problem

The SIMU configuration of Fig. 1 was modeled with the coefficients of Table 1 and subjected to the acceleration profile of Fig. 3. Each of the root-sum-square (RSS) values in Table 1 are composed of three equiaxially-distributed components. One exception exists; the initial platform misalignment about the z-platform (azimuth) axis is selected to be 1 arc min rather than the levelled axis values of 10 arc sec. To simplify computations, it was decided to simulate sightings on a star located along the y-platform axis. This selection permits calibration of drifts about the downrange and azimuth directions specified by the platform x-and z-axes, respectively, in Fig. 1.

Using an appropriately generated set of three H-matrices which reflect the staging instants in the profile of Fig. 3, the estimation performance of Table 2 was obtained. The greatest percentage uncertainty reduction is achieved with respect to initial platform misalignments. Nonetheless, after initial filtering, an improved calibration of the dominant errors is obtained and some improvement is subsequently obtained with respect to less dominant sources; e.g., platform deformation. From Table 2, it is possible to discern the essential effects of observation matrix-induced separability. The partial separability of gyro fixed drift (group 9) from mass unbalance terms (groups 10 and 11) is observed. The inseparability of platform misalignment (group 13) from servo errors (group 14) is evidenced by the effective masking of servo errors by the dominant misalignment terms; essentially no improvement in servo error sources is achieved.

Table 2 Uncertainty reduction after three filter passes[a]

Error groups	Initial value[b]	First pass[b]	Second pass[b]	Third pass[b]
1 through 8	See Table 1	Unchanged	Unchanged	Unchanged
9	0.1732	Unchanged	Unchanged	0.1730
10	0.1732	Unchanged	0.1726	0.1720
11	0.1732	Unchanged	0.1726	0.1720
12	0.0346	Unchanged	0.0345	0.0334
13	360	338	47.75	46.72
14	17.32	Unchanged	17.18	17.14
15	17.32	10.71	10.31	10.11
16	17.32	1.724	1.69	1.64
17	1.732	Unchanged	Unchanged	Unchanged
18	0	Unchanged	Unchanged	Unchanged

[a] No initial correlations; one-sigma observation noise equal to 20.5 arc sec.
[b] Three-axes RSS.

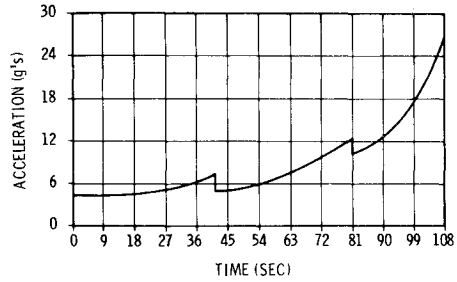

Fig. 3 Sample case acceleration profile.

Initial Conditions

Initial correlations between observable and unobservable errors can be induced by various preflight alignment schemes. In order to study the effects of various initial correlations it is desirable to obtain a measure of uncorrelated uncertainty reduction as a function of initial uncertainty magnitude. Table 3 was generated assuming that the alignment uncertainties about the platform level axes varied as shown: the initial launch azimuth uncertainty was one degree, and the stellar sighter error was 20 arc sec (1σ). The system configurations and acceleration-sighting sequence were identical to that used in generating Table 2. Error sources other than initial misalignments were set equal to zero.

Previously, the condition for estimation convergence of a virtually noiseless unobservable state estimation was shown to be that perfect correlation exist between observable and unobservable states. It is of practical interest to define the sensitivity of the sample-problem's state error statistics to induced correlations.

Consider groups 13, 17, and 18 of Table 1. That is, allow only the correlations initially existing between initial platform misalignment and initial position and velocity to vary. The initial (1σ) values for each of the element uncertainties are as follows: platform alignment about x-, y- and z-axes $=10$, 10, and 360 arc sec; position uncertainties $=100$ ft in three directions; velocity uncertainties $=100$ fps in three directions. The acceleration profile and system configurations previously discussed were employed to study three cases of various correlation relationships. The first case assumed that initial misalignment uncertainties are strongly correlated with initial position uncertainties only. The second case assumed that in addition to correlation between initial alignment and position error, significant correlation existed between position uncertainties and velocity errors at launch as well. Finally, the third case assumed that, in addition to the correlations existing between velocity and position errors in case two, perfect correlation was induced among position, velocity, and alignment initial errors.

Table 3 Effects of leveling errors on successive alignment estimates[a]

Level uncertainty[c] (arc sec)	Platform Uncertainty[b] Initial (arc sec)	Sighting 1 (arc sec)	Sighting 2 (arc sec)	Sighting 3 (arc sec)
0.00	3600.0	22.0	15.2	12.5
0.36	3600.0	22.0	15.3	12.5
3.60	3600.0	22.0	16.1	13.4
36.00	3600.0	45.9	41.6	39.9
360.00	3620.0	361.0	361.0	360.0
3600.00	6060.0	3600.0	3600.0	3600.0

[a] Initial azimuth alignment equals 3600 arc sec.
[b] Three-axes RSS.
[c] One-sigma observation noise equals 20.5 arc sec.

Table 4 Effects of initial correlation[a]

Parameter	Initial value (units)	Standard case sightings			Case 1 sightings			Case 2 sightings			Case 3 sightings		
		1	2	3	1	2	3	1	2	3	1	2	3
ω_x	10[b]	9	8	8	9	8	8	9	8	8	9	8	8
ω_y	10[b]	10	10	10	10	10	10	10	10	10	10	10	10
ω_z	360[b]	22	15	12	22	15	12	22	15	12	22	15	12
ω(RSS)	360[b]	25	20	18	25	20	18	25	20	18	25	20	18
P_x	100[c]	Unchanged			100	100	100	100	100	100	100	100	100
P_y	100[c]	Unchanged			91	84	78	91	84	78	91	84	78
P_z	100[c]	Unchanged			91	84	78	91	84	78	91	84	78
P(RSS)	173[c]	Unchanged			163	155	149	163	155	149	163	155	149
V_x	100[d]	Unchanged			Unchanged			Unchanged			91	84	78
V_y	100[d]	Unchanged			Unchanged			Unchanged			100	100	100
V_z	100[d]	Unchanged			Unchanged			Unchanged			100	100	100
V(RSS)	173[d]	Unchanged			Unchanged			Unchanged			168	164	162

[a] One-sigma observation noise equal to 20.5 arc sec. [b] arc sec; [c] ft; [d] fps.

For the conditions of the noted cases, Table 4 summarizes the resultant estimation performance. For the standard case, it is recalled that the observation matrix is insensitive to initial position and velocity errors. Hence, these elements are unobservable; they are not estimated. With the introduction of initial misalignment-initial position correlations in case one, however, observability is induced and estimation of initial position uncertainties is facilitated. In a similar manner, increased degrees of intercorrelation between (classically) observable and unobservable elements permits enhanced estimation; case three is an example.

Two additional aspects of Table 4 are worthy of comment. First, induction of correlations between an observable element and a correlation-induced observable element does not permit estimation of the former unobservable element unless it is also correlated with a strictly observable element. That is, correlation-induced observability is a one-stage relationship. Secondly, it is noted that although initial correlations improve the estimation of formerly unobservable elements; they do not corrupt the estimation of observable elements. The latter fact is a consequence of the algorithm's optimal character under conditions of complete observability.

To this point, all correlations between observable and correlation-induced observable state elements have been assumed equal to one. It is of interest to observe the effect of varying the level of correlation between elements in an attempt to discern tolerable levels of correlation for estimation purposes.

Figure 4 depicts the relation between ultimate a posteriori knowledge of the initial position error and initial correlation magnitudes. It is assumed that all correlations other than that between initial azimuth (ω_z) uncertainty and initial z-position uncertainty are zero. Figure 4 is essentially parabolic, indicating the need for relatively high correlations to gain moderately high estimation accuracy. Convergence is not absolute, but is within the accuracy of sighter noise.

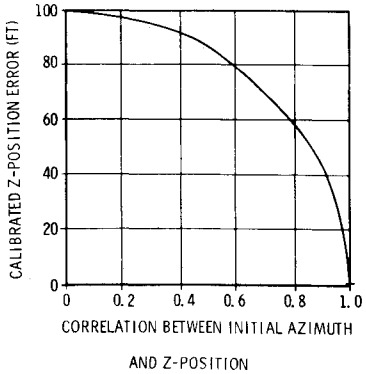

Fig. 4 Correlation effects on induced observability after three sightings.

Effects of Time-Varying Conditions

A heuristic discussion presents the issues of time-dependence related to the boost navigation problem. Assume that it is desired to estimate gyroscopic error parameters in the presence of a large initial misalignment and a large restraint drift uncertainty. If the first filter pass is made immediately after launch, the estimation procedure will effectively calibrate the constant initial misalignment values before sufficient time or acceleration has accumulated to permit restraint drift to camouflage the observable resulting from the initial misalignment.

In order to assess time-related effects independently of extraneous relationships (e.g., observability or noise), the data presented in Table 5 were generated using the error source group values given in Table 1. The table assumed a stellar sighting was taken every 10 sec of elapsed time throughout the boost phase.

Figure 5 depicts the time-varying behavior of aggregate estimated platform misalignment as well as its primary component, azimuth axis alignment uncertainty. Both curves display essentially identical characteristics since the azimuth uncertainty remains greater than twice the unobservable (and irreducible) y-axis uncertainty.

Although Table 5 and Fig. 5 adequately depict the time-varying nature of estimation results, the boost navigation problem is not likely to be without practical constrains which reduce the allowable number of star sightings to be taken during powered flight. Table 6 presents a summary of the aggregate (root-sum-square) uncertainty calibrations for different sighting sequences, assuming that sightings are performed only at booster staging. Two sets of assumptions were used to generate the table. The data in the left half of the table were generated under the assumption that only platform initial

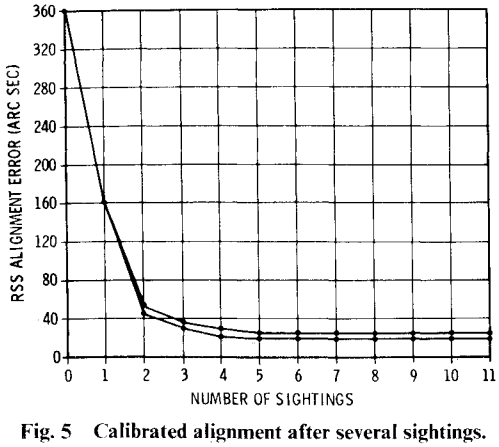

Fig. 5 Calibrated alignment after several sightings.

Table 5 Cumulative effects of several stellar sightings[a]

Error group	Sighting 0	1	2	3	4	5	6	7	8	9	10	11
Gyro:												
9	0.173	[b]	[b]	[b]	[b]	[b]	[b]	[b]	[b]	[b]	[b]	[b]
10	0.173	[b]	[b]	[b]	[b]	[b]	[b]	[b]	0.172	[b]	0.171	[b]
11	0.173	[b]	[b]	[b]	[b]	[b]	[b]	[b]	0.172	[b]	0.171	[b]
12	0.035	[b]	[b]	[b]	[b]	[b]	[b]	[b]	[b]	0.034	[b]	0.033
Platform:												
13	360	160	47	35	30	27	26	[b]	[b]	[b]	[b]	[b]
14	17	[b]	[b]	[b]	[b]	[b]	[b]	[b]	[b]	[b]	[b]	[b]
15	17	14	10	[b]	[b]	[b]	[b]	[b]	[b]	[b]	[b]	[b]
16	1.7	[b]	[b]	[b]	[b]	[b]	[b]	[b]	1.6	[b]	1.5	1.4

[a] One-sigma observation noise equals 20.5 arc sec.
[b] Unchanged from previous value.

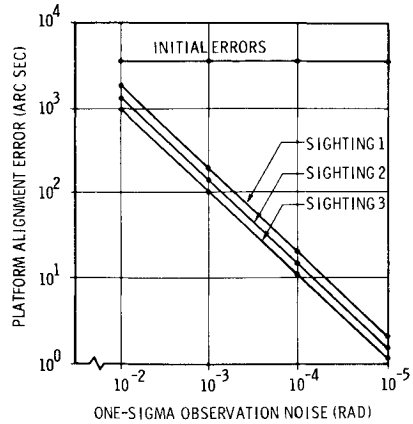

Fig. 6 Effects of observation noise.

misalignment contributes to the stellar observable; all other sources are assumed to be zero. In the right-hand half of the table, aggregate platform uncertainty is presented for conditions under which all error parameters cited in Table 1 are assumed operative.

Examination of the left-hand portion of Table 6 reveals that regardless of when sightings are performed, the effect on uncertainty reduction is unchanged. This is an obvious consequence of the observable-to-initial misalignment sensitivity's time invariance. Thus, in the absence of other than initial misalignment errors and with moderate sighter noise, the scheduling of sightings is irrelevant, only the number of sightings is significant. By contrast, in the presence of additional dynamic error sources, the relative desirability of unique sighting schedules becomes apparent.

Within Table 6, an optimum sighting policy can be discerned from the right-hand column conditions. It is most advantageous to obtain a sighting both early in flight and again near the end of booster operation; case number three. The rationale for the policy is that early sightings permit identification of acceleration-insensitive terms; subsequent sightings, following system exposure to the high acceleration environment serve to further the reduction of the initial misalignment uncertainty because of the increased separability of acceleration-sensitive terms.

Perhaps the most striking aspect of Table 6 is contained in row 7. It is noted that in the absence of other than platform initial misalignment terms, moderate improvement in platform alignment knowledge can be gained by performing repeated sightings after booster burnout. In the presence of acceleration-sensitive terms, of the magnitude given in Table 1, however, virtually no improvement in initial misalignment uncertainty is gained.

Table 6 Sighting sequence effects[a]

Sighting sequence (stage burnouts)	Platform misalignment (arc sec)[b]: Only initial misalignments active	All error parameters active
1	25	338
1, 2	25, 20	338, 48
1, 3	25, 20	338, 47
2, 3	25, 20	358, 78
3	25	360
1, 2, 3	25, 20, 18	338, 48, 47
Sequence of 3 Sightings after 3rd stage burnout	25, 20, 18	360, 360, 360

[a] Initial misalignments: $\omega_x = \omega_y = 10$ arc sec; $\omega_z = 360$ arc sec.
[b] Root-sum-square of three values.

Effects of Observation Noise

In the algorithm of Eqs. (8–13), use is made of the observation noise covariance matrix, R_k. The components of R_k are chosen to reflect the standard unit vector error inherent to the SIMU sensor. For purposes of numerical study, R_k is chosen to be diagonal with equal elements along its diagonal.

Figure 6 presents a summary of estimation accuracy as a nonlinear function of the observation noise variance. In order to isolate the effects of observation noise from extraneous contributors, only initial yaw platform misalignment was considered to contribute to the platform misalignment. That is, it is assumed that the platform is perfectly levelled prior to launch; sightings were performed at stage burnouts.

An appropriate description of the effect of observation noise on alignment estimation is that an order-of-magnitude improvement in observation accuracy results in an order-of-magnitude improvement in platform alignment estimation. If all error sources had been active, rather than only initial yaw misalignment, the rule of thumb deduced from the graph would necessarily apply to the total class of observable-producing error sources rather than yaw misalignment exclusively.

Conclusions

A relatively simple hardware device is shown to be analytically capable of performing sophisticated, large-scale error calibrations. Hardware capability is augmented via use of computational techniques. Choice of initial alignment technique and target star location strongly influence the effectiveness of the simple sighter for a given trajectory. System performance is functionally related to initial alignment conditions, sighter accuracy, and platform accuracy. Fundamental unobservability inherent to the SIMU hardware can be overcome by suitable induction of initial correlations among observable and unobservable error sources.

References

[1] Lichtenstein, B., "Gyros, Platforms, Accelerometers," *Kearfott Technical Information for the Engineer, No. 3*, 6th ed., Kearfott Division of General Precision Aerospace, N.J., June 1963, pp. 62–65

[2] Harter, G. A., "Error Analysis and Performance Optimization of Rocket Vehicle Guidance Systems," *Inertial Guidance*, edited by G. Pitman, Wiley, N.Y., 1962, pp. 294–328.

[3] Meditch, J. S., *Stochastic Optimal Linear Estimation and Control*, McGraw-Hill, San Francisco, 1971.

[4] Gura, I. A., "An Algebraic Solution of the State Estimation Problem," *AIAA Journal*, Vol. 7, No. 7, July 1969, pp. 1242–1247.